Research Square

Preprints are preliminary reports that have not undergone peer review.
They should not be considered conclusive, used to inform clinical practice,
or referenced by the media as validated information.

Exponential Convergence of Deep Composite Polynomial Approximation for Cusp-Type Functions

Kingsley Yeon

yeon@uchicago.edu

University of Chicago

Steven B. Damelin

zbMATH Open

Michael Werman

Hebrew University of Jerusalem

Research Article

Keywords:

Posted Date: November 11th, 2026

DOI: https://doi.org/10.21203/rs.3.rs-10373579/v1

License: This work is licensed under a Creative Commons Attribution 4.0 International License.
Read Full License

Additional Declarations: No competing interests reported.

Exponential Convergence of Deep Composite Polynomial Approximation for Cusp-Type Functions

Kingsley Yeon[1*], Steven B. Damelin[2] and Michael Werman[3]

[1*]Department of Statistics and CCAM, University of Chicago, Chicago, 60637, Illinois, USA.
[2]Department of Mathematics, zbMATH Open, Hermann-von-Helmholtz-Platz 1, Eggenstein-Leopoldshafen, 76344, Germany.
[3]Department of Computer Science, The Hebrew University of Jerusalem, Jerusalem, 91904, Israel.

*Corresponding author(s). E-mail(s): yeon@uchicago.edu;

Abstract

We investigate deep composite polynomial approximations of continuous but non-differentiable functions with algebraic cusp singularities. The functions in focus consist of finitely many cusp terms of the form $|\boldsymbol{x} - \boldsymbol{a_j}|^{\alpha_j}$ with rational exponents $\boldsymbol{\alpha_j} \in \boldsymbol{(0,1)}$ on a real-analytic background. We propose a constructive approximation scheme that combines a division-free polynomial iteration for fractional powers with an outer layer for analytic polynomial fitting. Our main result shows that this composite structure achieves exponential convergence under a balanced allocation of inner depth and outer degree. More precisely, the $\boldsymbol{L^p([-1,1])}$ approximation error decays exponentially both in the number of fitted scalar coefficients and in the size of the layered arithmetic graph, with these two budgets being linearly equivalent for the constructed sequence. This contrasts with the algebraic degree convergence of classical single-layer polynomial approximation for cusp-type functions. Numerical experiments for both single and multiple cusp configurations confirm the theoretical rates and demonstrate the parameter efficiency of deep composite polynomial constructions.

Keywords: deep polynomial approximation, composite polynomials, cusp singularities, fractional powers, exponential convergence

MSC Classification: 41A10 , 41A25 , 41A30 , 41A63

1 Introduction

A central problem in approximation theory is to approximate a given function f in a normed function space X by a simpler function $g \in X$ and to quantify the error $\|f - g\|_X$. The Weierstrass theorem asserts that every continuous function $f : [-1, 1] \to \mathbb{R}$ can be approximated uniformly by algebraic polynomials. It does not, however, determine the degree required to reach a prescribed accuracy. Quantitative approximation theory addresses this question by relating the approximation rate to the smoothness and singular structure of the target function.

Let Π_n denote the algebraic polynomials of degree at most n. For $f \in X$, define the best-approximation error

$$E_n(f)_X := \inf_{P \in \Pi_n} \|f - P\|_X.$$

For smooth functions, classical Jackson-type estimates give algebraic or faster rates as n increases. For functions with cusp singularities, however, a single global polynomial is limited by the local loss of differentiability. In this paper we study deep algebraic polynomial approximations of continuous, non-differentiable functions on $[-1, 1]$ and show that a layered polynomial representation can recover exponential convergence in a precisely defined representation budget; see Theorem 4.1.

The purpose of the present work is to demonstrate that deep composite polynomial constructions can substantially outperform classical single-layer polynomial approximation for a broad class of continuous functions with algebraic cusp singularities. Our approach combines a division-free polynomial iteration that resolves rational fractional powers with an outer analytic polynomial fit. The construction is explicit, uses only additions and multiplications, and yields a uniform exponential error bound. We distinguish throughout between the number of fitted coefficients, denoted by N_{train}, and the size of the complete layered arithmetic graph, denoted by N_{graph}. This distinction makes the exponential rate and the numerical comparisons unambiguous.

2 Degree of approximation

2.1 Notation

For $1 \le p < \infty$, write

$$\|f\|_p := \left(\int_{-1}^{1} |f(x)|^p \, dx \right)^{1/p}, \qquad \|f\|_\infty := \max_{x \in [-1,1]} |f(x)|.$$

For $0 < p < 1$, the same formula defines the usual L^p quasi-norm. For an integer $r \ge 1$, let $W_p^r([-1, 1])$ be the Sobolev space of functions whose $(r - 1)$st derivative is absolutely continuous and whose rth derivative lies in $L^p([-1, 1])$. We use

$$\|f\|_{W_p^r} := \|f\|_p + \|f^{(r)}\|_p.$$

We write $C^r([-1,1])$ for the space of r-times continuously differentiable functions and $C^\infty([-1,1])$ for the infinitely differentiable functions.

Throughout, $C, c, C_1, \ldots$ denote positive constants whose dependencies are stated when relevant. Their values may change from line to line.

2.2 Moduli of continuity

For $h > 0$ and an integer $r \geq 1$, define the forward differences recursively by

$$\Delta_h f(x) := f(x+h) - f(x), \qquad \Delta_h^r f := \Delta_h(\Delta_h^{r-1} f).$$

For $0 < h \leq 2/r$, the natural domain is $A_{rh} := [-1, 1 - rh]$. The rth modulus of smoothness is

$$\omega_r(f,t)_p := \sup_{0<h\leq \min\{t,2/r\}} \|\Delta_h^r f\|_{L^p(A_{rh})}.$$

When $r = 1$, we write $\omega(f,t)_p$.

2.3 Classical upper bounds

We recall two standard Jackson-type estimates; see [1, 2].

Theorem 2.1 *Let $r \geq 0$ be fixed and $1 \leq p \leq \infty$. If $f \in W_p^r([-1,1])$, then, for $n > r$,*

$$E_n(f)_p \leq C_{r,p}\, n^{-r} \omega\left(f^{(r)}, \frac{1}{n}\right)_p.$$

In particular, if $f \in W_p^1([-1,1])$, then

$$E_n(f)_p \leq C_p n^{-1} \|f'\|_p.$$

Theorem 2.2 *For each fixed integer $r \geq 1$ and $1 \leq p \leq \infty$, there is a constant $C_{r,p}$ such that*

$$E_n(f)_p \leq C_{r,p}\, \omega_r\left(f, \frac{1}{n}\right)_p, \qquad n \geq r.$$

If additionally $f \in W_p^r([-1,1])$, then

$$E_n(f)_p \leq C_{r,p}\, n^{-r} \|f^{(r)}\|_p.$$

3 Motivation

Our work builds on a line of research on deep composite polynomial approximation. The original motivation appeared in [3], which showed that composite polynomials formed by nesting low-degree polynomials can approximate non-smooth functions such as the absolute value with exponential convergence in the number of scalar quantities in the layered representation. This framework was extended to weighted approximation on unbounded domains in [4], where one-sided weights provide uniform control of functions with distinct two-sided behavior. Composite polynomials have also been studied

for efficient matrix-function evaluation and in settings where non-scalar multiplications dominate the computational cost [5, 6].

Algorithms that use only additions and multiplications are particularly relevant to homomorphic encryption, where computations are performed directly on encrypted data [7, 8]. This is important in privacy-sensitive applications such as cloud computing and secure data sharing [9, 10]. Cusp singularities also arise in applied problems. In physics and engineering they can describe critical geometric or constitutive behavior, including localized features in fluid interfaces and stress–strain relations [11]. In computer vision and graphics, cusp detection is relevant to contour analysis, object recognition, and feature-preserving geometric processing [12, 13].

4 Deep composite polynomial approximation for cusp-type continuous functions

Fix points $a_1, \dots, a_M \in [-1, 1]$ and rational exponents

$$\alpha_j = \frac{r_j}{s_j} \in (0, 1), \qquad r_j, s_j \in \mathbb{N}, \qquad s_j \geq 2.$$

Let $H : [-1, 1] \to \mathbb{R}$ be real analytic in a complex neighborhood of $[-1, 1]$. For each j, let h_j be real analytic in a complex neighborhood of $[0, 2^{\alpha_j}]$. Define

$$\mathcal{F} = \left\{ f(x) = H(x) + \sum_{j=1}^{M} h_j(|x - a_j|^{\alpha_j}) : x \in [-1, 1] \right\}. \tag{1}$$

Every $f \in \mathcal{F}$ is continuous and may fail to be differentiable at the points a_j.

4.1 Division-free inner iteration and outer analytic fit

Fix one exponent $\alpha = r/s \in (0, 1)$ and set $d := 2s$. For $t \in [0, 1]$, consider the division-free coupled iteration for the dth root [14]

$$\boxed{\begin{aligned} y_{k+1}(t) &= y_k(t)\Big(2 - d g_k(t)^{d-1} y_k(t)\Big), \\ g_{k+1}(t) &= g_k(t) - y_{k+1}(t)\Big(g_k(t)^d - t\Big), \end{aligned} \qquad g_0 \equiv 1, \quad y_0 \equiv \frac{1}{d}.} \tag{2}$$

Every update uses only additions and multiplications, so g_k and y_k are polynomials in t. For a cusp at $a \in [-1, 1]$, use the polynomial normalized variable

$$t_a(x) := \left(\frac{x - a}{2}\right)^2 \in [0, 1]$$

and define

$$\psi_{a,k}(x) := 2^{\alpha} g_k(t_a(x))^r. \tag{3}$$

Since $t_a(x)^{r/d} = (|x-a|/2)^{r/s}$, the target of (3) is $|x-a|^\alpha$. In particular, (3) is a genuine algebraic polynomial in x; no absolute-value operation is present in its evaluation graph.

4.1.1 Trainable-coefficient and graph budgets

For simplicity, take the same outer degree m and the same inner depth k for all cusp terms. The approximant constructed below has the form

$$G_{m,k}(x) = H_m(x) + \sum_{j=1}^{M} P_{j,m}\Big(\psi^{(j)}_{a_j,k}(x)\Big), \tag{4}$$

where H_m and each $P_{j,m}$ have degree at most m, and $\psi^{(j)}_{a_j,k}$ uses (2) with $d_j = 2s_j$.

We use two explicit notions of size.

First, the number of fitted scalar coefficients is

$$N_{\text{train}}(G_{m,k}) := (M+1)(m+1). \tag{5}$$

The cusp locations a_j, rational exponents r_j/s_j, and constants in the root iteration are fixed problem data and are therefore not counted as trainable coefficients.

Second, $N_{\text{graph}}(G_{m,k})$ is the size of a straight-line arithmetic graph evaluating $G_{m,k}$: one node is counted for each stored fitted coefficient and for each scalar addition or multiplication. Powers with fixed integer exponents are evaluated by a fixed multiplication scheme. Since M and the integers r_j, s_j are fixed, there are constants $c_-, c_+ > 0$, independent of m and k, such that

$$c_-\big((M+1)(m+1) + Mk\big) \le N_{\text{graph}}(G_{m,k}) \le c_+\big((M+1)(m+1) + Mk\big). \tag{6}$$

Thus, for a fixed function class, $N_{\text{graph}} = \Theta(m+k)$ when M is fixed. A classical degree-n polynomial has $n+1$ fitted coefficients and can be evaluated by Horner's rule with $\Theta(n)$ arithmetic nodes. Consequently, comparison at equal N_{train} or equal N_{graph} is meaningful up to fixed implementation constants. The generally much larger degree of the fully expanded composite polynomial is not used as the complexity budget, because the approximant is stored and evaluated in its layered form.

Theorem 4.1 (Exponential convergence in both budgets) *Let $f \in \mathcal{F}$ be fixed and let $0 < p \le \infty$. There exist constants $C, c > 0$ and a sequence of deep composite polynomials G_ℓ such that*

$$\|f - G_\ell\|_{L^p([-1,1])} \le Ce^{-c\ell}, \qquad N_{\text{train}}(G_\ell) = \Theta(\ell), \qquad N_{\text{graph}}(G_\ell) = \Theta(\ell). \tag{7}$$

Equivalently, after changing the constants, the error is exponentially small in either the fitted-coefficient budget or the complete graph budget:

$$\|f - G_\ell\|_{L^p([-1,1])} \le C_{\text{train}} e^{-c_{\text{train}} N_{\text{train}}(G_\ell)}, \tag{8}$$

$$\|f - G_\ell\|_{L^p([-1,1])} \le C_{\text{graph}} e^{-c_{\text{graph}} N_{\text{graph}}(G_\ell)}. \tag{9}$$

The constants may depend on the analytic neighborhoods and bounds of $H, h_1, \dots, h_M$, on the cusp data (a_j, r_j, s_j), on M, and on p, but not on ℓ.

Proof We first prove a uniform exponential estimate for the inner iteration. Fix $t \in [0,1]$, set $u = t^{1/d}$, and suppress the t-argument. Define

$$z_k := d g_k^{d-1} y_k, \qquad A_k := z_k(2 - z_k).$$

The reciprocal update in (2) gives

$$d g_k^{d-1} y_{k+1} = A_k. \tag{10}$$

Notice that this identity uses g_k on both sides; replacing the left-hand side by $d g_{k+1}^{d-1} y_{k+1}$ would be incorrect.

Define

$$F_d(z) := z(2-z)\left(1 - \frac{z(2-z)}{d}\right)^{d-1}, \qquad 0 \le z \le 1.$$

Because $F_d'(0) = 2 > 1$ and $F_d(1) = (1 - 1/d)^{d-1} < 1$, continuity gives a number $\delta_d \in (0,1)$ such that $F_d(\delta_d) = \delta_d$. Moreover, writing $a = z(2-z)$, one has

$$\frac{d}{da}\left[a\left(1 - \frac{a}{d}\right)^{d-1}\right] = \left(1 - \frac{a}{d}\right)^{d-2}(1-a) \ge 0, \qquad 0 \le a \le 1,$$

so F_d is increasing on $[0,1]$.

We now prove by induction that

$$u \le g_k \le 1, \qquad \delta_d \le z_k \le 1 \qquad (k \ge 0). \tag{11}$$

The assertion holds at $k = 0$ because $g_0 = 1$ and $z_0 = 1$. Assume it holds at step k and set $q_k = u/g_k \in [0,1]$. From (2) and (10),

$$\frac{g_{k+1}}{g_k} = 1 - \frac{A_k}{d}(1 - q_k^d). \tag{12}$$

Consequently,

$$z_{k+1} = A_k\left[1 - \frac{A_k}{d}(1 - q_k^d)\right]^{d-1}. \tag{13}$$

Since $0 < A_k \le 1$, equation (13) gives $z_{k+1} \le 1$. It also gives

$$z_{k+1} \ge A_k\left(1 - \frac{A_k}{d}\right)^{d-1} = F_d(z_k) \ge F_d(\delta_d) = \delta_d.$$

Finally, using $1 - q_k^d = (1 - q_k)(1 + q_k + \cdots + q_k^{d-1})$, we obtain the exact error identity

$$g_{k+1} - u = (g_k - u)\left[1 - \frac{A_k}{d}\left(1 + q_k + \cdots + q_k^{d-1}\right)\right]. \tag{14}$$

The bracket is nonnegative because $A_k \le 1$ and the geometric sum is at most d. Moreover, (12) gives $g_{k+1} \le g_k \le 1$. Hence $u \le g_{k+1} \le 1$, completing the induction.

Let

$$\vartheta_d := 1 - \frac{\delta_d(2 - \delta_d)}{d} \in (0,1).$$

Since the geometric sum in (14) is at least 1 and $A_k \ge \delta_d(2 - \delta_d)$, we have

$$0 \le g_k(t) - t^{1/d} \le \vartheta_d^k \qquad \text{uniformly for } t \in [0,1]. \tag{15}$$

The map $v \mapsto v^r$ is r-Lipschitz on $[0,1]$, so (3) and (15) imply

$$\big\| |x-a|^\alpha - \psi_{a,k}(x) \big\|_{L^\infty([-1,1])} \le 2^\alpha r\, \vartheta_d^k. \tag{16}$$

This estimate is uniform up to the cusp and requires no boundary-layer argument.

We next approximate the analytic outer functions. For each j, analyticity of h_j in a complex neighborhood of $[0, 2^{\alpha_j}]$ implies that there are constants $B_j > 0$, $R_j > 1$, and degree-m polynomials $P_{j,m}$ such that

$$\|h_j - P_{j,m}\|_{L^\infty([0,2^{\alpha_j}])} \le B_j R_j^{-m}. \tag{17}$$

Markov's inequality on $[0, 2^{\alpha_j}]$ and the uniform boundedness of $\|P_{j,m}\|_\infty$ give

$$\|P'_{j,m}\|_\infty \le D_j m^2, \tag{18}$$

where D_j is independent of m. Combining (16)–(18) yields

$$\left\| h_j\big(|x - a_j|^{\alpha_j}\big) - P_{j,m}\Big(\psi^{(j)}_{a_j,k}(x)\Big) \right\|_\infty \le B_j R_j^{-m} + E_j m^2 \vartheta_{2s_j}^k. \tag{19}$$

Similarly, analyticity of H gives degree-m polynomials H_m and constants $B_0 > 0$, $R_0 > 1$ such that

$$\|H - H_m\|_\infty \le B_0 R_0^{-m}.$$

Define $G_{m,k}$ by (4). Because M and the cusp exponents are fixed, (19) gives constants $C > 0$, $R > 1$, and $\vartheta \in (0, 1)$ such that

$$\|f - G_{m,k}\|_\infty \le C\left(R^{-m} + m^2 \vartheta^k\right). \tag{20}$$

Choose a fixed $\gamma > 0$ and set $m = \lfloor \gamma k \rfloor$. Absorbing the polynomial factor m^2 into a slightly slower exponential gives

$$\|f - G_{m,k}\|_\infty \le C' e^{-c'k}. \tag{21}$$

By (5) and (6), this balanced choice satisfies

$$N_{\text{train}}(G_{m,k}) = \Theta(k), \qquad N_{\text{graph}}(G_{m,k}) = \Theta(k).$$

Taking $k = \ell$ proves (7) and (8) for the uniform norm. For $0 < p < \infty$,

$$\|f - G_{m,k}\|_p \le 2^{1/p} \|f - G_{m,k}\|_\infty,$$

which proves the result for every $0 < p \le \infty$. □

Remark 4.2 The same construction applies on any finite interval $[A, B]$ after an affine change of variables.

4.1.2 Interpretation of the exponential parameter

The exponential variable in Theorem 4.1 is not the degree of the fully expanded polynomial. It is either the fitted-coefficient count N_{train} or the complete layered graph size N_{graph}. Under the balanced choice $m \asymp k$, these quantities are linearly equivalent, and therefore the same constructed sequence has exponential decay in both. This also makes the comparison with a classical degree-n polynomial fair at the level of storage and arithmetic complexity: such a polynomial has $n+1$ fitted coefficients and a Horner graph of size $\Theta(n)$.

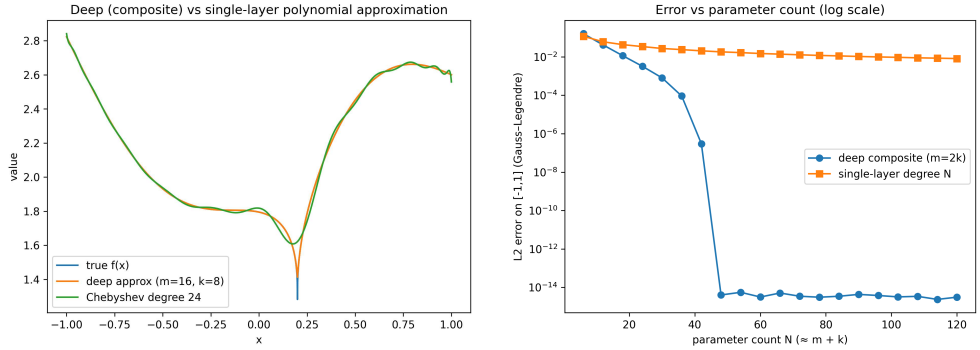
For plots it is convenient to suppress implementation-dependent constants and use the normalized proxy

$$\widehat{N}_{\text{graph}} := m + k \quad \text{for one cusp}, \qquad \widehat{N}_{\text{graph}} := M(m + k) \quad \text{for } M \text{ cusp terms}. \tag{22}$$

Equation (6) shows that $\widehat{N}_{\text{graph}}$ and N_{graph} differ only by fixed multiplicative and additive constants when the exponents and M are fixed. Hence semilog slopes against $\widehat{N}_{\text{graph}}$ represent the same exponential law, although absolute operation counts depend on the chosen power-evaluation implementation.

4.2 One-dimensional numerical illustrations

Figures 1 and 2 illustrate the approximation behavior of the proposed deep composite polynomial model for functions with algebraic cusp singularities. In Figure 1, we consider a single cusp located at $a = 0.2$ with exponent $\alpha = r/s = 1/3$, where the target function has the form $f(x) = H(x) + h(|x - a|^{\alpha})$ with an analytic envelope h. The left panel shows a representative approximation using parameters (m, k), while the right panel plots the $L^2([-1, 1])$ error, computed via Gauss–Legendre quadrature, against the normalized graph proxy $\widehat{N}_{\text{graph}} = m + k$. A classical polynomial baseline of degree proportional to the same budget has both a comparable coefficient count and a comparable Horner-graph size, up to fixed constants. Figure 2 shows analogous results for multiple cusps, using the proxy $\widehat{N}_{\text{graph}} = M(m + k)$. In both cases, the observed semilog behavior is consistent with the exponential-in-N_{graph} convergence proved above.



(a) Approximation of a cusp-type function (b) Pointwise absolute error (log scale)

Fig. 1 Comparison of approximants for a cusp-type function. The rate plot uses the normalized graph proxy $\widehat{N}_{\text{graph}} = m + k$; fixed arithmetic-node constants are omitted.

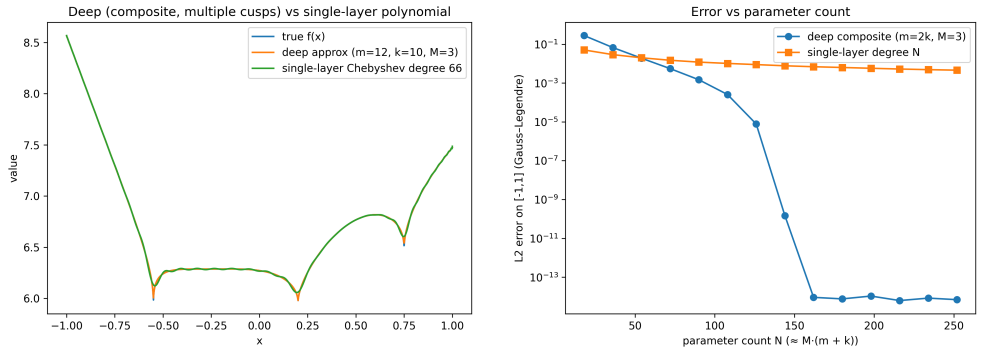
4.3 Two-dimensional level-set illustrations

We also illustrate the approximation of one-dimensional angular cusp profiles inside two-dimensional level-set visualizations. These examples retain the polar-coordinate map and the outer hyperbolic tangent, so the full displayed map is not claimed to be an algebraic polynomial in (x, y); the polynomial approximation is applied to the angular radial profile. Let $(x, y) \in [-1, 1]^2$, define polar coordinates

$$r = \sqrt{x^2 + y^2}, \qquad \theta = \operatorname{atan2}(y, x) \in (-\pi, \pi],$$

and construct a star-shaped domain through a radial profile $R_\star(\theta)$. Specifically, we consider

$$R_\star(\theta) = R_0 + \sum_{j=0}^{K_\star - 1} W_j \exp\big(-\lambda_j \, |\theta - \theta_j|^{\alpha_j}\big),$$



(a) Approximation of a multiple-cusp function (b) Pointwise absolute error (log scale)

Fig. 2 Comparison of approximants for a multiple-cusp function. The rate plot uses the normalized graph proxy $\widehat{N}_{\mathrm{graph}} = M(m+k)$.

where $K_\star$ denotes the number of star tips, θ_j are their angular locations, $W_j > 0$ their amplitudes, $\lambda_j > 0$ decay rates, and $\alpha_j \in (0,1)$ control the sharpness of the angular cusps. The associated level-set function is

$$f(x,y) = \tanh\big(\gamma\,(R_\star(\theta) - r)\big),$$

so that the zero contour $f = 0$ traces a simply connected star whose boundary is smooth away from the tips and exhibits algebraic angular cusps at $\theta = \theta_j$.

We first consider a symmetric five-point star with $K_\star = 5$, equally spaced spike locations $\theta_j = \theta_0 + 2\pi j/5$, and a fixed cusp exponent $\alpha_j = 1/3$ for all j (Figure 3). We approximate $R_\star(\theta)$ using the analogous deep composite architecture for the one-dimensional angular variable: a division-free inner root map approximates the fractional powers $|\theta - \theta_j|^{\alpha_j}$, and outer Chebyshev polynomials of degree m fit the resulting envelopes.

With $m = 20$ and $k = 15$, the deep model has $N_{\mathrm{train}} = K_\star(m+1) = 105$ fitted outer coefficients. Its normalized complete-graph proxy is $\widehat{N}_{\mathrm{graph}} = K_\star((m+1)+k) = 180$, before fixed operation weights are assigned. The displayed Chebyshev baseline has degree 104 and is therefore matched to the fitted-coefficient count $N_{\mathrm{train}} = 105$, not to the larger complete graph budget. This coefficient-matched comparison isolates parameter efficiency, while an operation-matched comparison would use a classical degree proportional to $\widehat{N}_{\mathrm{graph}}$. On a 400×400 grid over $[-1,1]^2$, the deep composite approximation attains an L^2 error of 3.17×10^{-3}, compared to 3.55×10^{-2} for the coefficient-matched Chebyshev baseline.

We next consider an uneven eight-point star with $K_\star = 8$, where the spike locations θ_j are randomly perturbed from uniform spacing and the parameters α_j, W_j, and λ_j vary across tips, producing nonuniform cusp sharpness and asymmetric geometry (Figure 4). Using $m = 22$ and $k = 16$ gives $N_{\mathrm{train}} = K_\star(m+1) = 184$ and normalized graph proxy $\widehat{N}_{\mathrm{graph}} = K_\star((m+1)+k) = 312$. The deep composite model achieves an L^2 error of 9.74×10^{-3} on a 420×420 grid, compared to 2.40×10^{-2} for the coefficient-matched Chebyshev approximation. Despite the increased geometric irregularity, the

composite model consistently captures localized cusp behavior more accurately than the global polynomial baseline.

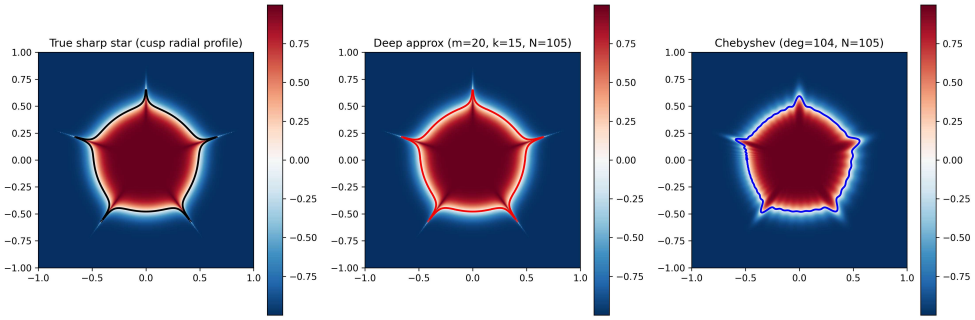


Fig. 3 Sharp five-point star with algebraic angular cusps. Left: true level set $f(x, y) = \tanh(\gamma(R_\star(\theta) - r))$ (black); middle: deep composite approximation ($K_\star = 5$, $m = 20$, $k = 15$, $N_{\text{train}} = 105$, normalized graph proxy $\widehat{N}_{\text{graph}} = 180$, red); right: coefficient-matched Chebyshev baseline of degree $D = 104$ (blue). The L^2 errors are 3.17×10^{-3} for the deep model and 3.55×10^{-2} for the Chebyshev baseline on a 400×400 grid.

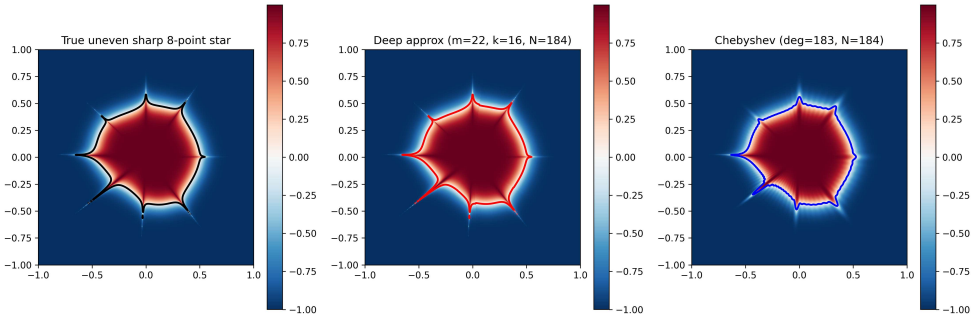


Fig. 4 Uneven eight-point star with algebraic angular cusps. Left: true level set; middle: deep composite approximation ($K_\star = 8$, $m = 22$, $k = 16$, $N_{\text{train}} = 184$, normalized graph proxy $\widehat{N}_{\text{graph}} = 312$); right: coefficient-matched Chebyshev baseline, with zero contours shown in black, red, and blue.

5 Conclusion

We have given a constructive deep polynomial approximation scheme for analytic backgrounds perturbed by finitely many rational algebraic cusps. The division-free inner iteration admits a uniform contraction estimate on the full normalized interval, including the singular endpoint, and the outer analytic fits converge geometrically. Balancing inner depth and outer degree produces exponential convergence in both the number of fitted coefficients and the complete layered graph size. The explicit distinction between N_{train} and N_{graph} also separates coefficient-matched numerical

comparisons from operation-matched comparisons. The numerical examples illustrate the advantage over matched single-layer Chebyshev approximations in both one- and two-dimensional cusp geometries. Natural extensions include irrational cusp exponents, adaptive allocation of depth across nonuniform singularities, and stability analysis in finite precision.

Declarations

Funding

Not applicable.

Competing interests

The authors declare no competing interests.

Ethics approval and consent to participate

Not applicable.

Consent for publication

Not applicable.

Data availability

No external datasets were used in this study. The numerical results are generated from the test functions specified in the manuscript.

Materials availability

Not applicable.

Code availability

Code may be provided by the corresponding author upon reasonable request.

Author contributions

All authors contributed to the conception, analysis, and writing of the manuscript and approved the final version.

References

[1] DeVore, R.A., Lorentz, G.G.: Constructive Approximation. Grundlehren der mathematischen Wissenschaften 303, Springer-Verlag, ??? (1993)

[2] Mhaskar, H.N., Pai, D.V.: Fundamentals of Approximation Theory. Alpha Science International, Oxford U.K, ??? (2007)

[3] Yeon, K.: Deep univariate polynomial and conformal approximation. arXiv preprint arXiv:2503.00698 (2025)

[4] Yeon, K., Damelin, S.B.: On uniform weighted deep polynomial approximation. arXiv preprint arXiv:2506.21306 (2025)

[5] Jarlebring, E., Sastre, J., Ibáñez, J.: Polynomial approximations for the matrix logarithm with computation graphs. Linear Algebra and its Applications **721**, 692–714 (2025)

[6] Yeon, K., Ghosal, P., Anitescu, M.: Bolt: Block-orthonormal lanczos for trace estimation of matrix functions. arXiv preprint arXiv:2505.12289 (2025)

[7] Rivest, R.L., Adleman, L., Dertouzos, M.L.: On data banks and privacy homomorphisms. Foundations of secure computation (1978)

[8] Gentry, C.: Homomorphic encryption: a mathematical survey. EMS Press (2022). Accessed: 2024-09-26

[9] Authors, M.: Fully Homomorphic addition and multiplication. Accessed: 2024-09-26 (2025)

[10] Acar, A., Aksu, H., Uluagac, A.S., Conti, M.: A survey on homomorphic encryption schemes: Theory and implementation. ACM Computing Surveys **51**, 1–35 (2018)

[11] Callister, W.D., Rethwisch, D.G.: Materials Science and Engineering: An Introduction, 10th edn. Wiley, ??? (2018)

[12] Szeliski, R.: Computer Vision: Algorithms and Applications. Springer, ??? (2010)

[13] Koenderink: Solid Shape vol. 2. MIT Press, ??? (1990)

[14] Blanchard, J.D., Chamberland, M.: Newton's method without division. The American Mathematical Monthly **130**(7), 606–617 (2023)